

Shear Flow Past An Inclined Square Cylinder

Sachin Saurabh, sachin.saurabh07@gmail.com

Lecturer, Department of mechanical engineering, Assosa

University, Ethiopia, 8271732022/+251989428048, Sachin.saurabh07@gmail.com

Abstract

Steady incompressible flow past a square cylinder inclined at 45° is numerically investigated by using finite-element formulation in two-dimensions. The discretized equations are solved by GMRES (Generalized Minimal RESidual method). The computations are carried out in the Reynolds number (Re) range of 5- 40 using a blockage of 0.05 and a shear parameter of 0.01 and 0.02. Dirichlet type boundary conditions are employed on the side walls along with the shear inlet and stress-free exit. One may expect, due to shear inlet, asymmetry in the cylinder wake. As a result, the cylinder wake was observed to be slightly asymmetric and the onset of separation is in between $Re = (5, 10)$. The drag force, as expected, decreases with Re in the steady regime. Interestingly, the cylinder also experiences a small value of lift (-0.0451) at $Re = 5$, result of shear provided at the inlet, which increases monotonically to -0.0274 as Re reaches 40. The symmetric surface pressure plot (expected to be asymmetric) illustrates that the base pressure becomes locally maximum from locally minimum with increase in Re. This is in contrast with those obtained for circular cylinder where the base pressure is always locally maximum. Different values of shear parameter and its effect on flow behaviour and characteristics is a part of further studies.

Keywords: stabilized finite-element, shear parameter, blockage

1. Introduction

In spite of extensive experimental and numerical studies on flow past a bluff bodies, shear flow past an inclined square cylinder is very useful for many practical applications, e.g. vortex flowmeters, buildings, bridges, towers, and wires. At very low Re, the flow is laminar, steady and does not separate from the cylinder. With the increasing Re, the flow separates from the trailing edge but remain steady and laminar up to Re of about 40. Beyond this Re, the flow undergoes a time dependent periodically oscillating wake. We are performing the numerical simulation in the range Re 5-40 for shear parameters ($k= 0.01$ 0.02) at a blockage(b) of 0.05. Cheng et al. [2007] numerically simulated shear flow around square cylinder, examined vortex shedding frequency and aerodynamic forces exerted on the cylinder for Re ranging from 100 to 200 and K ranging from 0.0 to 0.5 using lattice Boltzmann method. Their results show that vortex phenomenon is strongly dependent on Re and K. The experimental studies are done by Kiya et al. [1980] to investigate the flow phenomenon. They reported that for shear flows, the critical Reynolds number (Re_c) above which the vortex shedding occurs is higher than the Re_c for uniform flows. Robert R.Hwang [1997] studied the shear effect on vortex shedding behind a square cylinder, he solved 2D N-S equations using a finite difference method. His results show the effect of shear rate on the incoming flow on the vortex shedding, lift and drag forces in the range of $K = 0.0$ to 0.25 and Re from 500 1500.

2. The governing equations

2.1 The incompressible flow equations

Let $\Omega \subset \mathbb{R}^{nsd}$ be the spatial domain, where $nsd = 2$ is the number of space dimensions and $(0, T)$ be the temporal domain. The boundary of Ω is denoted by Γ and is assumed to be piecewise smooth. The closure of the domain is denoted by $\bar{\Omega}$. The spatial and temporal coordinates are denoted by x and t , respectively. The equations governing the unsteady flow of an incompressible fluid are:

$$\rho \left(\frac{\partial u}{\partial t} + u \cdot \nabla u \right) - \nabla \cdot \sigma = 0 \text{ on } \Omega \times (0, T), \quad (1)$$

$$\nabla \cdot u = 0 \text{ on } \Omega \times (0, T). \quad (2)$$

Here u and σ denote the fluid velocity and the Cauchy stress tensor, respectively. The stress is the sum of its isotropic and deviatoric parts:

$$\sigma = -pI + T, \quad T = 2\mu \varepsilon(u), \quad \varepsilon(u) = \frac{1}{2}(\nabla u + (\nabla u)^T) \quad (3)$$

where p , I , μ and ε are the pressure, identity tensor, dynamic viscosity of the fluid and strain rate tensor,

respectively. Both, the Dirichlet and Neumann-type boundary conditions are accounted for and are represented as

$$u = g \text{ on } \Gamma_g, \quad n \cdot \sigma = h \text{ on } \Gamma_h, \quad (4)$$

respectively, where Γ_g and Γ_h are complementary subsets of the boundary Γ , n is its unit normal vector and h is the surface traction vector. The initial condition on the velocity is specified on Ω at $t = 0$:

$$u(x, 0) = u_0 \text{ on } \Omega, \quad (5)$$

where u_0 is divergence-free, i.e. u_0 satisfies Equation (2). The momentum equation for steady incompressible flow is obtained by dropping the time-derivative in Equation (1).

3 The finite-element formulation

The spatial domain Ω is discretized into non-overlapping sub-domain $\Omega^e = 1, 2, \dots, n_{el}$ where n_{el} is the number of elements. S_u^h and S_p^h be the finite dimensional trial function spaces for velocity and pressure, respectively and the corresponding weighting function spaces are denoted by r_u^h and r_p^h . these function spaces are defined as:

$$S_u^h = \{u^h | u^h \in [H^1(\Omega)]^2, u^h = 0 \text{ on } \Gamma_{gl}\}, \quad (6)$$

$$ruu^h = 1w^h | w^h \in [H^{1h}(\Omega)]^2, w^h = 0 \text{ on } \Gamma_{gl}. \quad (7)$$

$$Sp^h = r_p^h = 1q^h | q^h \in H^{1h}(\Omega), \quad (8)$$

$$\text{where } H^{1h} = 1\phi^h | \phi^h \in C^0(\Omega), \phi^h \in P^1V\Omega^e. \quad (9)$$

Here, P^1 represents the first degree polynomials. Thus, over the element domain, this space is formed by using first degree polynomials in space and time. Globally, the interpolation functions are continuous in space but discontinuous in time. The stabilized space-time formulation for deforming domains is then written as follows:

$$\begin{aligned} \text{given } (u^h)_n, \text{ find } u^h \in (Suu^h)_n \text{ and } p^h \in (Sp^h)_n \text{ such that } \int_{\Omega} w^h \cdot \rho (\partial_{u^h} \partial t + u^h \cdot \nabla V) u^h - \\ f^j d\Omega + \int_{\Omega} \epsilon \epsilon(w^h) : \sigma \sigma(p^h, u^h) d\Omega + \int_{\Omega} q^h \nabla V \cdot u^h d\Omega + \sum_{e \in \mathcal{E}_h} \int_{\rho e=1} [e (\partial_{w^h} \partial t)^j + u^h \cdot \nabla V] w^h - \\ \nabla V \cdot \sigma \sigma(q^h, w^h) \cdot \rho 1_p \tau (\partial_{u^h} \partial t + u^h \cdot \nabla V) u^h - f^j - \nabla V \cdot \sigma \sigma(p^h, u^h) d\Omega + \int_{\Omega} e^{\delta V V \cdot w^h} \rho \nabla V \cdot u^h d\Omega \\ = \int (\tau_{n,h} w^h \cdot h^h) d\tau \end{aligned}$$

In the variational formulation as given above, the first three terms and the right hand side constitute the Galerkin formulation of the problem. The first series of element level integrals in Equation (10) are the SUPG (streamline-upwind/Petrov-Galerkin) and the PSPG (pressure-stabilizing/Petrov-Galerkin) stabilization terms added to the variational formulations of the momentum and the continuity equations, respectively. At high Re, in an advection dominated flow, the Galerkin formulation of the flow equations lead to node-to-node oscillations in the velocity field. This numerical instability is overcome by adding the SUPG stabilization contribution to all the terms of the Galerkin weak form of the momentum equations. The SUPG formulation for convection 4

4 Problem description

4.1 Problem set-up

An inclined square cylinder of Diameter D is placed mid-way between two lateral walls of a channel which are at a distance of H apart, as shown in Figure 4.1. The flow is described in a Cartesian coordinating system (x and y) in which the x -axis is in the direction of inlet flow direction (i.e. in stream wise direction), while y -axis is normal to the x -axis (cross-stream direction). The origin is centered at the mid point of the upstream face of the cylinder. The flow characteristics are such that the fluid enters the channel with a linear profile and the lateral walls are assigned with no-slip condition on velocity, i.e. the velocity is set to zero at upper and lower boundaries. Neumann condition for velocity is applied on downstream boundary that corresponds to stress-free condition.

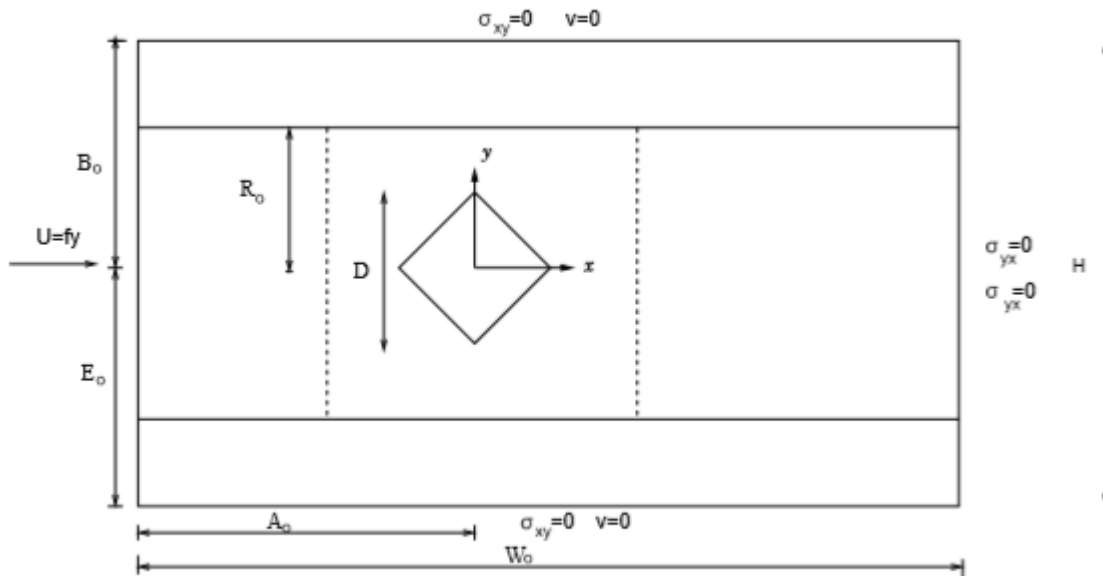


Figure 1: Problem set-up for flow past an inclined square cylinder.

4.2 The finite-element mesh

A finite-element mesh used for computing the flow past an inclined square cylinder is shown in Figure 4.2.

The distances of the upstream and downstream boundaries from the origin of the cylinder are denoted by L_u and L_d , respectively. In the present work, $L_u = 60D$ and $L_d = 150D$. The mesh is structured, non-uniform and consists of 90418 nodes and 89700 elements. Figure 2: Finite-element mesh for simulating flow past an inclined square cylinder at 5% blockage with 90418 nodes and 89700 elements.

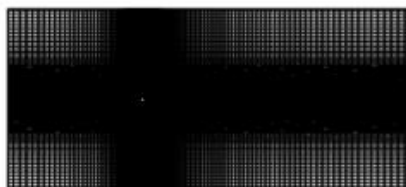


Figure 2: Finite-element mesh for simulating flow past an inclined square cylinder at 5% blockage with 90418 nodes and 89700 elements.

5 .Results

The present study is done by numerically solving the equations of flow and motion. The results are presented for $Re=5,10,20,30,40$ and $Re=100$. The computations are done for a two dimensional flow with $B = 6$ $\sigma_{yx=0}$ $\sigma_{yx=0} \sigma v=0$ $\sigma 0.05$. Various post processing tools were used to extract the data from the files generated by FORTRAN code.

5.1 Development of steady separation bubble with Re

Development of the steady separation bubble is determined by streamline contour plots with Re. streamlines are plotted for $Re=5,10,20,30,40$. It is observed that no separation bubble is formed for Re 5 . The separation bubble between the Reynolds no 5-10.The bubble once formed continuously enlarges with increase in Re.

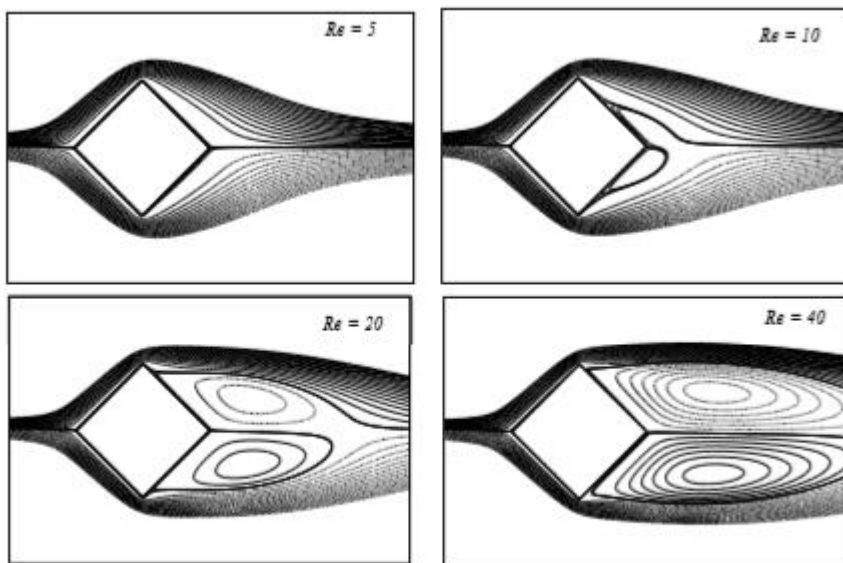


Figure 3: streamline plot for Re 5, 10, 20 and 30 for shear parameter $k=0.01$

5.2 Variation of drag and lift coefficient with Re

Variation of drag and lift coefficient is shown in figure with Re. It is observed that drag coefficient of shear flow past an inclined square cylinder at a blockage of $B = 0.05$, in steady flow is high at low Re which further decreases with increase in Re "

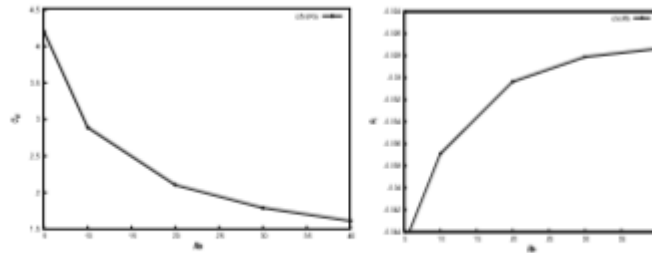


Figure 4: variation of drag and lift coefficients with Re 5, 10, 20, 30 and 40

5.3 Surface pressure distribution

Surface pressure distribution is shown in figure from $Re = 5-40$ for laminar flow past an inclined square cylinder. The pressure coefficient C_p is computed using no-slip boundary conditions on cylinder surface. It

has been observed that The symmetric surface pressure plot (expected to be assymmetric) illustrates that the base pressure becomes locally maximum from locally minimum with increase in Re . This is in contrast with those obtained for circular cylinder where the base pressure is always locally maximum.

The symmetric surface pressure plot (expected to be assymmetric) illustrates that the base pressure becomes locally maximum from locally minimum with increase in Re . This is in contrast with those obtained for circular cylinder where the base pressure is always locally maximum.

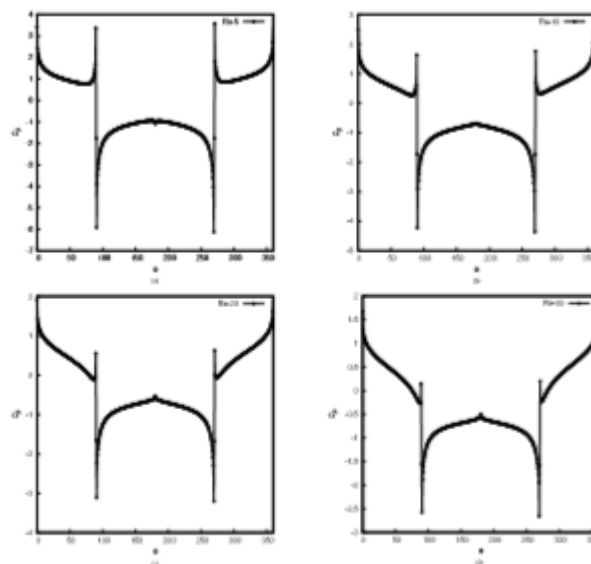


Figure 5: surface pressure plot for Re 5, 10, 20 and 30

6. Conclusions

A stabilized finite element formulation using Streamline Upwind/Petrov Galerkin (SUPG) and Pressure stabilized/Petrov Galerkin (PSPG) method with great accuracy is used. A parabolic flow with no-slip boundary condition at lateral walls, and shear free condition at downstream are used. It is observed that drag coefficient decreases with increase in Re , while lift coefficient increase with increase in Re . steady separation of bubbles occurs in the range Re 5-10. surface pressure plot is symmetric for Re range 0-40 for shear parameter $k=0.01$ and $k=0.02$. The base pressure becomes locally maximum from locally minimum with increase in Re .

Reference

- [1] **M. Cheng, S. H. N. Tan, K. C. Hung**, Linear shear flow over a square cylinder at low reynolds number. physics of Fluids, 17:078103, 1994.
- [2] **D.S. Whyte, J. Lou**. Numerical simulation of flow around a square cylinder in uniform shear flow. Journal of Fluids and Structures ,207-226, 2007.
- [3] **H. Tamura and M. Arie**. Vortex shedding from a circular cylinder in moderate reynolds number shear flow. Journal of Fluid Mechanics, 721-735, 1980.
- [4] **Y. C. Sue, 1997**, Numerical simulation of shear effect on vortex shedding behind a square cylinder. International Journal for Numerical Methods in Fluids, 1409-1420, 1997.
- [5] **S. Vengadesan** Onset of vortex shedding in planar shear flow past a square cylinder, 1054-1059.. International Journal of Heat and Fluid Flow, 1054-1059, 2008.
- [6] **S. Vengadesan** Shear effect on square cylinder wake transition characteristics, International Journal for Numerical Methods in Fluids. International Journal for Numerical Methods in Fluids , 67,1112-1134,2010.
- [7] **Rajendra kr.ray**. Numerical Study of Shear Flow Past a Square Cylinder at Reynolds Numbers. Proceeding Engineering , 127, 102-109, 2015.

A Brief Author Biography

Sachin Saurabh– Presently working as a lecture in department of mechanical engineering, Assosa university, Ethiopia M.tech(Spl in Thermal Engineering) From Indian Institute of Technology(ISM) Dhanbad and also having five years of teaching experience. My research area of interest is fluid mechanics and computational Fluid Dynamics(CFD) due to its various mode of solutions to solve realistic fluid flow problems.